

## REPORT

## METALLURGY

# Bone-like crack resistance in hierarchical metastable nanolaminate steels

Motomichi Koyama,<sup>1\*</sup> Zhao Zhang,<sup>1</sup> Meimei Wang,<sup>2,3\*</sup> Dirk Ponge,<sup>2</sup> Dierk Raabe,<sup>2</sup> Kaneaki Tsuzaki,<sup>1</sup> Hiroshi Noguchi,<sup>1</sup> Cemal Cem Tasan<sup>3,\*</sup>

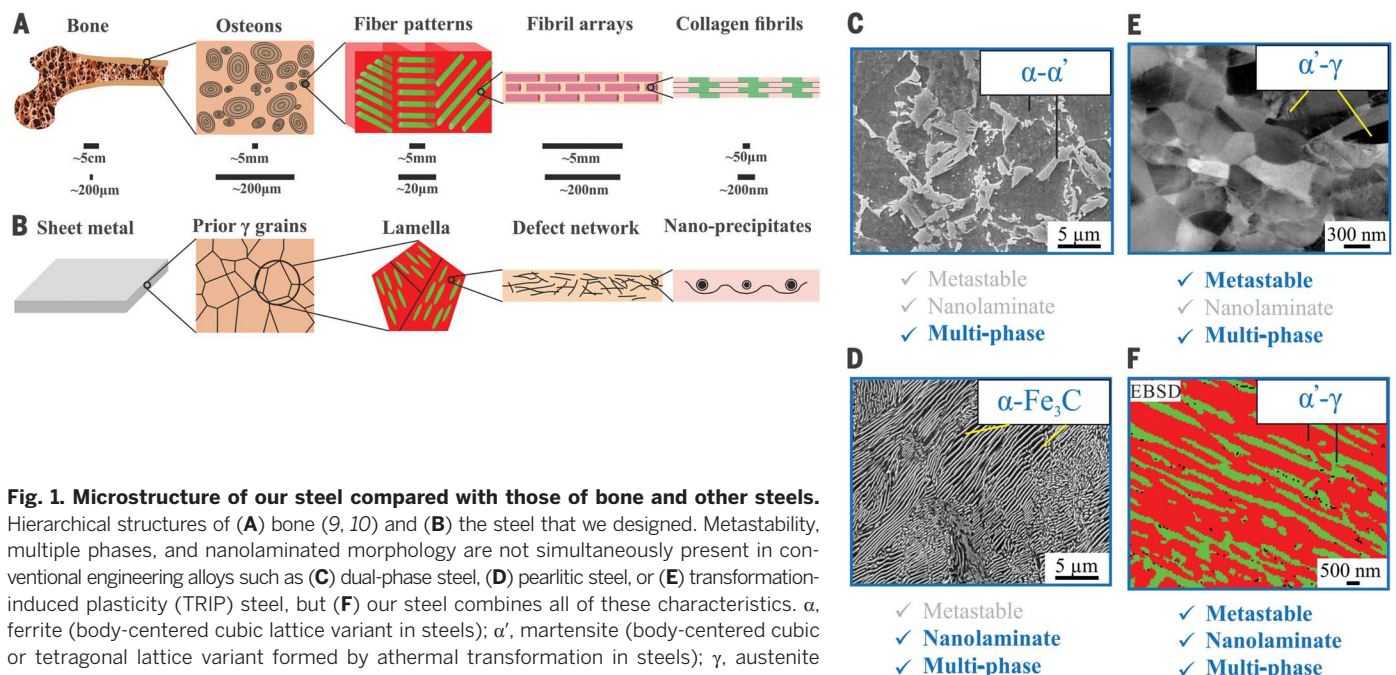
Fatigue failures create enormous risks for all engineered structures, as well as for human lives, motivating large safety factors in design and, thus, inefficient use of resources. Inspired by the excellent fracture toughness of bone, we explored the fatigue resistance in metastability-assisted multiphase steels. We show here that when steel microstructures are hierarchical and laminated, similar to the substructure of bone, superior crack resistance can be realized. Our results reveal that tuning the interface structure, distribution, and phase stability to simultaneously activate multiple micromechanisms that resist crack propagation is key for the observed leap in mechanical response. The exceptional properties enabled by this strategy provide guidance for all fatigue-resistant alloy design efforts.

**W**hen components of engineered systems such as trains, planes, spacecraft, or power plants fail, human life is at risk. Because cyclic loads often cause these failures, fatigue resistance is the main failure prevention goal in component design. Fatigue is a materials phenomenon (1–3), but it is mostly dealt with by using large safety factors in design (4, 5), rather than by applying

materials solutions. This is due to the fact that the latter often cannot compensate for the intrinsically large statistical variations observed in fatigue life (6, 7). To this end, in pursuit of exceptional improvements in fatigue resistance, we were inspired by the excellent fracture toughness of bone (despite its intrinsic difference from fatigue resistance) (8). The substructure of bone is hierarchical and lam-

inated, which leads to superior crack resistance by simultaneous activation of multiple micromechanisms that resist crack propagation (9, 10). We hypothesized that (i) a similar response can be transferred to metals by designing a hierarchical and nanolaminated multiphase microstructure to benefit from interface structure (11, 12) and distribution (13, 14) effects, and (ii) this resistance can be further enhanced by rendering the microstructure metastable to benefit from well-tuned and local phase transformation mechanisms (15, 16). The overall goal is the simultaneous activation of roughness-induced crack termination (RICT) and transformation-induced crack termination (TICT) mechanisms. The steels that we explored to investigate the validity of this hypothesis (e.g., Fe<sub>9</sub>Mn<sub>3</sub>Ni<sub>1.4</sub>Al, in weight percent) have an intrinsic hierarchical structure that is comparable to that of bone (Fig. 1A) and composed of laminated martensite and metastable austenite phases (17, 18) (Fig. 1, B and F). Thus, they possess the key combination of three characteristics—namely, multiple phases, metastability, and nanolamination.

Figure 2 reveals the exceptional fatigue limit and fatigue life of these multiphase metastable nanolaminate steels under cyclic mechanical

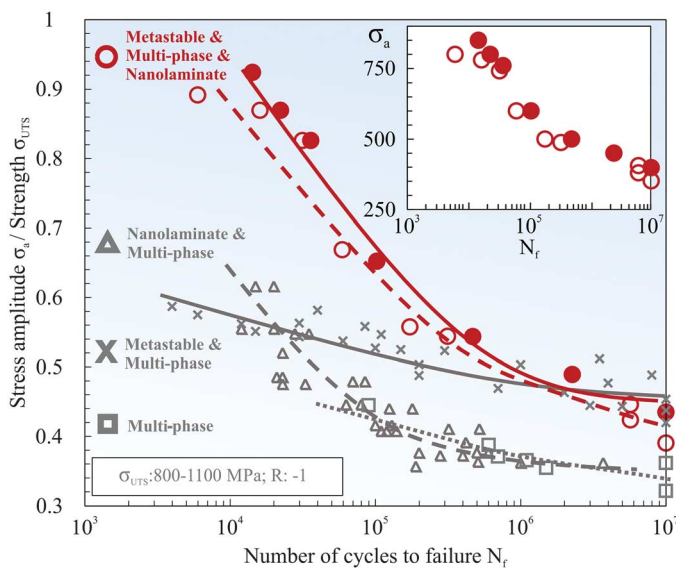


<sup>1</sup>Kyushu University, Motooka 744, 819-0395 Fukuoka, Japan.

<sup>2</sup>Max-Planck-Institut für Eisenforschung, Max-Planck-Straße 1, 40237 Düsseldorf, Germany. <sup>3</sup>Department of Materials Science and Engineering, Massachusetts Institute of Technology, 77 Massachusetts Avenue, Cambridge, MA 02139, USA.

\*Corresponding author. Email: koyama@mech.kyushu-u.ac.jp (M.K.); mm\_wang@mit.edu (M.W.); tasan@mit.edu (C.C.T.)

**Fig. 2. Number of cycles to failure, plotted against stress amplitude.** The stress amplitude is normalized by the ultimate tensile strength (UTS) of the steels shown in Fig. 1 (33–36). The open and solid red circles indicate the results for the steels aged at 873 K for 1 and 8 hours, respectively; the inset shows the non-normalized data.  $R_c$ , stress ratio.



loading with respect to conventional steels of different compositions and subjected to thermomechanical processing [details are given in (19)] that do not simultaneously exhibit these three characteristics (Fig. 1, C to E). To verify that the crucial factor in the observed fatigue

behavior is the targeted presence of multiple micromechanisms of crack termination, we (i) systematically discuss the fatigue performance of this new alloy generation relative to that of conventional high-strength steels (Figs. 1 and 2) and (ii) provide microstructural and

mechanical proof of crack termination mechanisms (Figs. 3 and 4).

We start with a typical automotive high-strength steel: Ferrite-martensite dual-phase (DP) steel (Fig. 1C) shows relatively low fatigue limits (Fig. 2) (20, 21). We attribute this performance to the absence of effective crack termination mechanisms that could hamper crack growth and the high mechanical contrast between the soft ferrite phase and the hard martensite phase (22). In fact, efforts for developing better design strategies against crack propagation (23) were originally motivated by the need to render such high-strength and -formability multiphase steels more fatigue-resistant. Ferrite-cementite pearlitic steel (cementite,  $Fe_3C$ ; Fig. 1D), on the other hand, shows improved fatigue resistance in comparison with the DP steel (Fig. 2). In this steel, the multiphase nanolaminate microstructure morphology, which is different from the globular structure of DP steel, deflects fatigue cracks constantly during growth, thereby introducing a friction stress acting on the crack surface and decelerating the fatigue crack opening and growth process (24, 25). Thus, this improvement is due to the RICT mechanism. It has been demonstrated elsewhere to be affected by the morphological characteristics of the cementite network, such as the interlamellar spacing (24) and lamellar alignment (26). The fatigue limit of pearlitic steel is low, because the RICT mechanism does not work efficiently for the deceleration of small cracks (27). Metastable multiphase martensite-austenite transformation-induced plasticity (TRIP) steel (Fig. 1E) also shows an improved fatigue resistance compared with DP steel (Fig. 2). The formation of compressive residual stress fields, arising from the volume-expanding transformation from face-centered cubic  $\gamma$ -austenite to body-centered cubic (or body-centered tetragonal)  $\alpha'$ -martensite at the crack tip (25, 28, 29), suppresses crack initiation and growth (30). Thus, we attribute the enhancement, as well as the higher strength-ductility balance for the multiphase TRIP steel, to the TICT mechanism. However, similar to the RICT effect on fatigue life discussed above, the effects of TRIP and TICT are stress amplitude-dependent (Fig. 2). Their contributions are less effective when the stress amplitude is high, because an increasing stress amplitude leads to larger plastic strain, which in turn results in a decrease in the fraction of metastable  $\gamma$ -austenite via transformation (18) during the early loading cycles. The improvements in the fatigue performance of our metastable multiphase nanolaminate steel with respect to that of these conventional steels provide an indirect confirmation of the simultaneous introduction of the RICT and TICT (and TRIP) effects. Another indirect corroboration was given when we modified our steel to have a different, less ideal microstructure, which indeed led to inferior fatigue properties (fig. S4).

The alloy presented here is not yet specifically optimized for the best possible fatigue

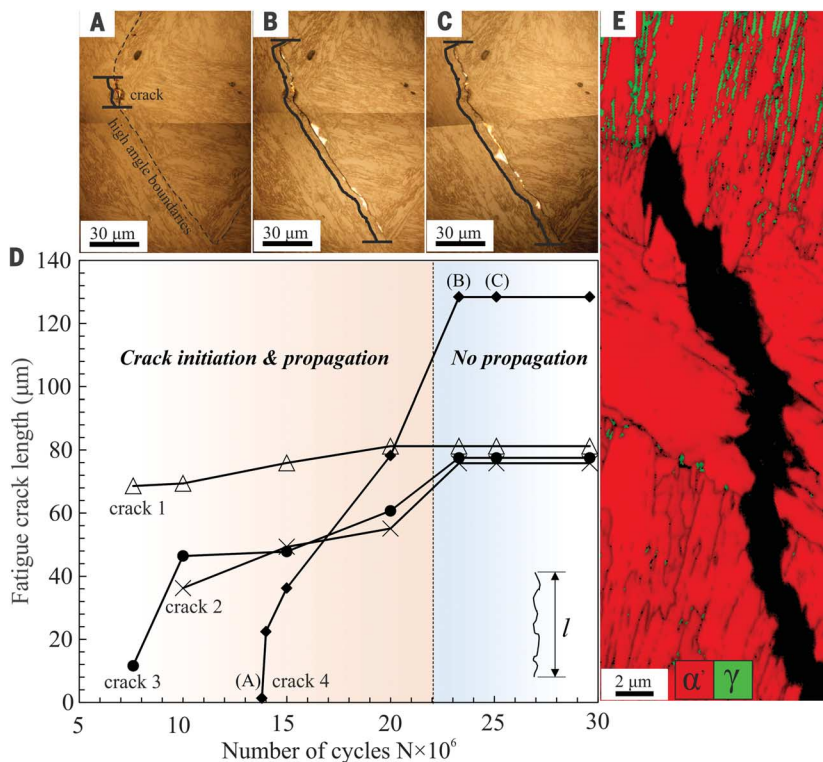


**Fig. 3. Optical images of a replicated specimen surface at the fatigue limit of the metastable multiphase nanolaminate steel aged for 1 hour.** (A) Crack initiation, (B) crack propagation, and (C) crack nonpropagation. (D) Corresponding crack propagation and nonpropagation behavior of the four cracks observed; the crack behavior indicated by diamonds is for the crack shown in (A) to (C).  $l$ , crack length. (E) EBSD phase map showing transformation in the vicinity of the fatigue crack.

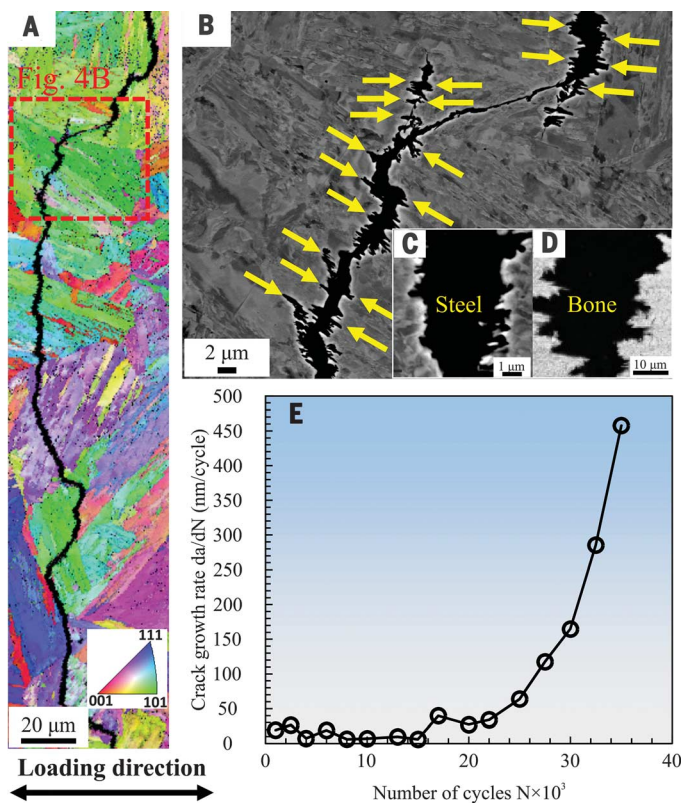


**Fig. 4. Hierarchical roughness on the 760-MPa fatigue crack in the metastable multiphase nanolaminate steel aged for 1 hour.**

(A) EBSD imaging. (B) Electron channeling contrast imaging. (C) Magnified image of the microroughness on the fracture. (D) Similarity of a fracture in human bone (8). (E) Propagation rate of the fatigue crack shown in (A) and (B). a, crack length.

performance in the case of high cycle numbers. With improved inclusion control (Fig. S2) (31) and especially with thermodynamic and kinetic optimization for achieving a wider range of austenite stability (32), we expect further enhancement of the fatigue properties, particularly in the high-cycle fatigue regime. In fact, a difference in the fatigue limit is evident if the mechanical properties and thickness of the austenite films are changed by aging for a different duration (solid versus open circles in Fig. 2).

Next we focus on the mechanisms: A replica study for fatigue cracks developing at the fatigue limit confirms that crack initiation (Fig. 3A) is delayed until  $10^7$  cycles and that the small cracks grow slowly at the highest cycling (Fig. 3, B to D). The delayed fatigue crack initiation and the hampering of its propagation are key factors for improving the fatigue limit. We find that the arrest of crack propagation takes place in both directions (parallel and perpendicular to lath alignment) when the cracks reach prior austenite boundaries (Fig. 3C), which are the interfaces decorated by austenite films in this steel (Fig. 1F) (18). These boundaries undergo substantial local hardening and residual compressive stress induced by the transformation of the austenite films (i.e., the TICT effect) in the vicinity of the fatigue crack (Fig. 3E).

In contrast, at high stress amplitudes, fatigue cracks form at the early stages of the test and then continuously propagate until macroscopic failure. However, the fatigue crack

propagation path is deflected when propagating across or along different grain boundaries or the lamellae (Fig. 4A). The crack surface morphology exhibits many small branches, indicated by the yellow arrows in Fig. 4B. The microroughness on the crack surface, enabled by the laminate's hierarchical microstructure morphology (Fig. 1B), enhances the RICT effect. This mechanism decelerates fatigue crack growth even at a late fatigue stage (Fig. 4E), providing superior fatigue life at high stress amplitudes. The marked similarity of the observed fracture process to the fracture of bone (8), despite the obvious difference in the constitution of these two materials, provides another demonstration of the success of the proposed approach (Fig. 4, C and D).

We conceived and demonstrated the effectiveness of a metastable multiphase nanolaminate microstructure concept for creating materials with exceptional fatigue resistance. This is achieved by simultaneously enabling transformation-induced and roughness-induced crack termination mechanisms. The demonstrated superior low-cycle fatigue life and high fatigue limit constitute essential progress for steels, and we expect similar improvements in material properties for any alloys that can be designed with similar microstructures. Thus, this strategy has potential to improve the safety of advanced structures and components that experience cyclic loads.

#### REFERENCES AND NOTES

1. Y. D. Wang *et al.*, *Nat. Mater.* **2**, 101–106 (2003).

2. D. S. Kemsley, *Nature* **178**, 653–654 (1956).
3. H. Mughrabi, *Acta Mater.* **61**, 1197–1203 (2013).
4. S. Timoshenko, *History of Strength of Materials: With a Brief Account of the History of Theory of Elasticity and Theory of Structures* (Courier Corporation, 1953).
5. C. M. Sonsino, *Int. J. Fatigue* **29**, 2246–2258 (2007).
6. K. S. R. Chandran, *Nat. Mater.* **4**, 303–308 (2005).
7. A. Pineau, D. L. McDowell, E. P. Busso, S. D. Antolovich, *Acta Mater.* **107**, 484–507 (2016).
8. H. Peterlik, P. Roschger, K. Klaushofer, P. Fratzl, *Nat. Mater.* **5**, 52–55 (2006).
9. R. K. Nalla, J. H. Kinney, R. O. Ritchie, *Nat. Mater.* **2**, 164–168 (2003).
10. R. O. Ritchie, *Nat. Mater.* **10**, 817–822 (2011).
11. L. L. Li, Z. J. Zhang, P. Zhang, Z. G. Wang, Z. F. Zhang, *Nat. Commun.* **5**, 3536 (2014).
12. L. L. Li, P. Zhang, Z. J. Zhang, Z. F. Zhang, *Sci. Rep.* **4**, 3744 (2014).
13. Z. Ma *et al.*, *Sci. Rep.* **6**, 22156 (2016).
14. Y. Kimura, T. Inoue, F. Yin, K. Tsuzaki, *Science* **320**, 1057–1060 (2008).
15. Y.-B. Ju, M. Koyama, T. Sawaguchi, K. Tsuzaki, H. Noguchi, *Acta Mater.* **112**, 326–336 (2016).
16. B. Gludovatz *et al.*, *Science* **345**, 1153–1158 (2014).
17. M. M. Wang, C. C. Tasan, D. Ponge, A. Kostka, D. Raabe, *Acta Mater.* **79**, 268–281 (2014).
18. M. M. Wang, C. C. Tasan, D. Ponge, A. C. Dippel, D. Raabe, *Acta Mater.* **85**, 216–228 (2015).
19. Materials and methods are available as supplementary materials.
20. J. A. Wasynczuk, R. O. Ritchie, G. Thomas, *Mater. Sci. Eng.* **62**, 79–92 (1984).
21. Z. G. Hu, P. Zhu, J. Meng, *Mater. Des.* **31**, 2884–2890 (2010).
22. X.-L. Cai, J. Feng, W. S. Owen, *Metall. Trans. A Phys. Metall. Mater. Sci.* **16**, 1405–1415 (1985).
23. S. Suresh, R. O. Ritchie, *Int. Met. Rev.* **29**, 445–475 (1984).
24. G. T. Gray, J. C. Williams, A. W. Thompson, *Metall. Trans. A Phys. Metall. Mater. Sci.* **14**, 421–433 (1983).
25. R. O. Ritchie, *Mater. Sci. Eng. A* **103**, 15–28 (1988).
26. I. Verpoest, E. Aernoudt, A. Deruyttere, M. De Bondt, *Int. J. Fatigue* **7**, 199–214 (1985).
27. M. A. Daeubler, A. W. Thompson, I. M. Bernstein, *Metall. Trans. A Phys. Metall. Mater. Sci.* **21**, 925–933 (1990).
28. H. R. Mayer, S. E. Stanzl-Tschegg, Y. Sawaki, M. Hühner, E. Hornbogen, *Fatigue Fract. Eng. Mater. Struct.* **18**, 935–948 (1995).
29. Z. Mei, J. W. Morris Jr., *Eng. Fract. Mech.* **39**, 569–573 (1991).
30. A. G. Pineau, R. M. Pelloux, *Metall. Trans.* **5**, 1103–1112 (1974).
31. Y. Murakami, S. Kodama, S. Konuma, *Int. J. Fatigue* **11**, 291–298 (1989).
32. G. N. Haidemenopoulos *et al.*, *Mater. Sci. Eng. A* **573**, 7–11 (2013).
33. A. Aran, H. Türker, *J. Mater. Sci. Lett.* **9**, 1407–1408 (1990).
34. M. Abareishi, E. Emadoddin, *Mater. Des.* **32**, 5099–5105 (2011).
35. G. T. Gray, A. W. Thompson, J. C. Williams, *Metall. Trans. A Phys. Metall. Mater. Sci.* **16**, 753–760 (1985).
36. T. Fujisawa *et al.*, *Int. J. Fract.* **185**, 17–29 (2014).

#### ACKNOWLEDGMENTS

This work was financially supported by KAKENHI (Grants-in-Aid for Scientific Research from the Japan Society for the Promotion of Science; 15K18235 and 16H06365), the European Research Council (ERC) under the European Union's 7th Framework Programme (FP7/2007–2013, ERC Advanced Grant agreement 290998), and the Department of Materials Science and Engineering of the Massachusetts Institute of Technology. C.C.T. and M.K. designed the research; Z.Z. and M.W. were the lead experimental scientists; and M.K. and C.C.T. wrote the paper. All authors discussed the results and commented on the manuscript. The authors declare no conflicts of interest.

#### SUPPLEMENTARY MATERIALS

www.sciencemag.org/content/355/6329/1055/suppl/DC1  
Materials and Methods  
Supplementary Text  
Figs. S1 to S8  
Tables S1 and S2  
References (37–46)

25 October 2016; accepted 10 February 2017  
10.1126/science.aal2766



**Bone-like crack resistance in hierarchical metastable nanolaminate steels**

Motomichi Koyama, Zhao Zhang, Meimei Wang, Dirk Ponge, Dierk Raabe, Kaneaki Tsuzaki, Hiroshi Noguchi and Cemal Cem Tasan (March 9, 2017)

*Science* **355** (6329), 1055-1057. [doi: 10.1126/science.aal2766]

Editor's Summary

**Bone-inspired steel**

Load cycling of metal components leads to fatigue and ultimately failure through the propagation of cracks. Koyama *et al.* took inspiration from bone to develop a steel with a laminated substructure that arrests cracks. The resulting hierarchical material has much better fatigue resistance properties than other iron alloys. The strategy need not be limited to steel; other metal alloys should also benefit from this type of microstructural engineering.

*Science*, this issue p. 1055

---

This copy is for your personal, non-commercial use only.

---

**Article Tools** Visit the online version of this article to access the personalization and article tools:  
<http://science.sciencemag.org/content/355/6329/1055>

**Permissions** Obtain information about reproducing this article:  
<http://www.sciencemag.org/about/permissions.dtl>

*Science* (print ISSN 0036-8075; online ISSN 1095-9203) is published weekly, except the last week in December, by the American Association for the Advancement of Science, 1200 New York Avenue NW, Washington, DC 20005. Copyright 2016 by the American Association for the Advancement of Science; all rights reserved. The title *Science* is a registered trademark of AAAS.